Electronic Supplementary Information

Strong Coupling effect induced surface reconstruction of CeF_3-Ni_3N to form CeF_3-NiOOH for oxygen evolution reaction

*Rajdeep Kaur, †Ashish Gaur, † Jatin Sharma, Vikas Pundir, Aashi and Vivek Bagchi**

Institute of Nano Science and Technology, Sector-81, Knowledge City, Sahibzada Ajit Singh Nagar, Punjab, Pin - 140306, India

†both the authors contributed equally

Table of Contents

S1.1 Physical characterization:

The physical characterization of the as-prepared CeF_3-Ni_3N was done using various techniques. First of all, bya Bruker Eco D8 ADVANCED X powder X-ray diffractometer consisting of a Ni filter was used for its initial steps of examination. The radiations of CuK (=1.5405, 40 KV and 25 mA) was used for the study. The examination was done in the 2Ɵ range of 20°- 80° and step size of about 0.0020/step was given. Scanning electron microscope from JEOL (JSM 17-300) was used for studying the morphology of the catalyst. The energy-dispersive X-ray diffractometer (Bruker) study was also done by the same scanning electron microscope. The complete information about the structure of CeF_3-Ni_3N and the average particle size was measured by Transmission electron microscope (TEM) JEOL-2100 which was operated at 200 KV. X-ray photoelectron spectroscopy (XPS) on ECSA: 220-IXL with MgKα is used for further investigation of elements. The MgKα used is non-monochromated X-ray beam with photon energy 1253.6 eV.

S1.2. Electrochemical Analysis:

All the electrochemical measurements were carried out in CHI 760E electrochemical workstation. In the three-electrode system, saturated Ag/AgCl electrode is used as a reference electrode and a Graphitic rod as a counter electrode. Firstly, the prepared electrode was used for taking all the polarization data at a scan rate 5 mV s^{-1} in 1 M KOH. After all the polarization data was collected, it was converted to Reversible hydrogen electrode (RHE) by the use of equation $E_{RHE} = E_{Ag/AgCl} + 0.197 + 0.059*pH$. For the calculation of Tafel slope, polarisation curves were again plotted, and the linear region of Tafel plot was fitted to the Tafel equation i.e., $\eta = b \log(j) + a$. The electrochemical surface area (ECSA) was determined by the calculation of double layer capacitance, in which CV scans of the as prepared electrode were taken at a scan rate of 20 to 200 mV/s in 1M KOH in non-faradaic potential range. when ΔJ = (Janodic-Jcathodic)/2 was plotted against the scan rate at a potential of 1.08 V vs RHE and was fitted linearly, it gave the value of double layer capacitance (Cdl). The faradic efficiency was calculated by taking the ratio of experimental and theoretical oxygen evolution in the reaction.

S2.1. PXRD spectra of as synthesized CeF_3 and Ni_3N:

The PXRD pattern was obtained in the 2θ angular region of 20° to 80° with an increment of 0.0020/Step.

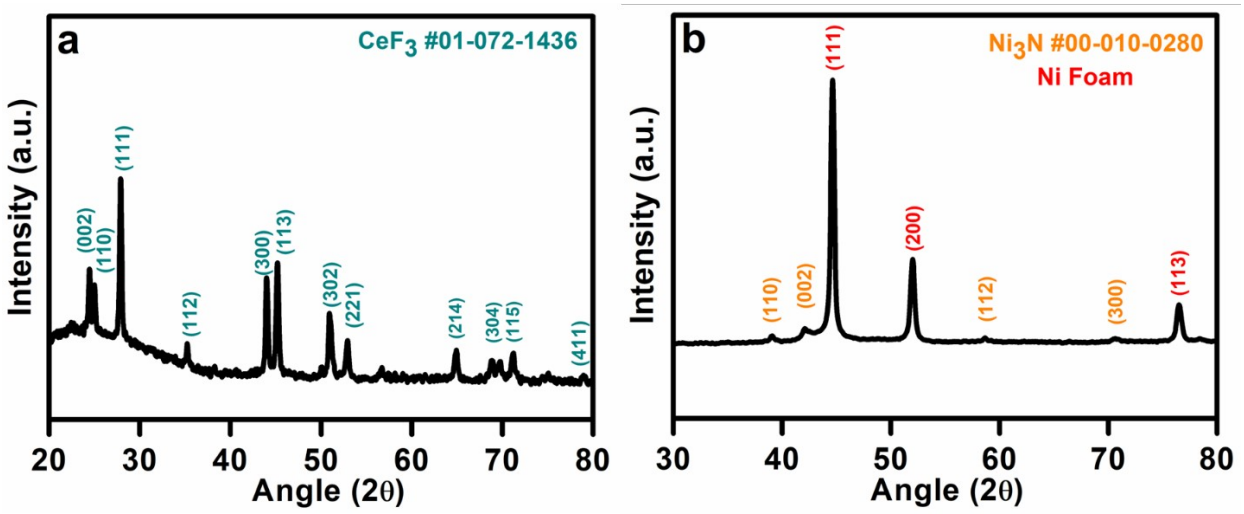

Figure S1. PXRD pattern of CeF_3 and Ni_3N

S2.2. XPS wide range spectra of Ni_3N and CeF_3:

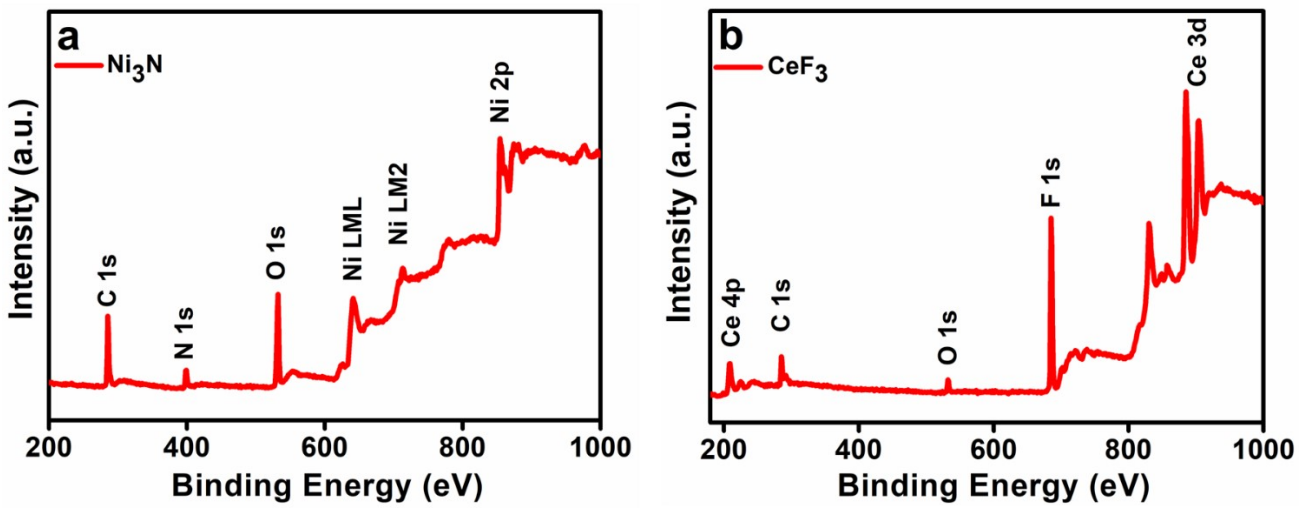

Figure S2. XPS wide angle spectrum of Ni_3N and CeF_3 consisting of Ni, N, Ce and F elements present in the catalyst.

S2.3. XPS spectra of NiOOH:

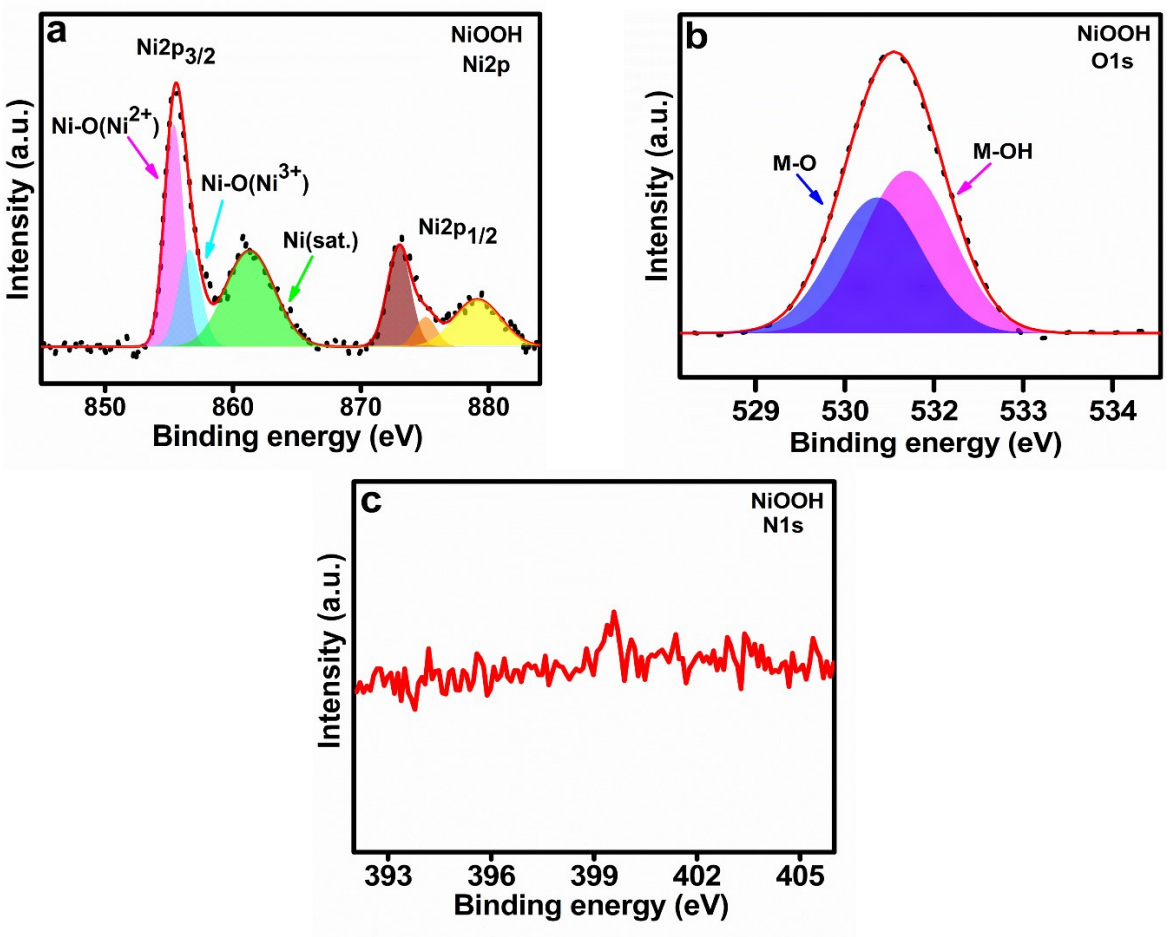

Figure S3. XPS High resolution spectra of NiOOH consisting of Ni, N, and O elements present in the catalyst.

S3.1. Reference table:

S. No.	Catalyst Name	Electrolyte	Overpotential (mV)	Tafel Slope (mV/dec)	Reference
1.	Ni_3N/Ni Foam	1M KOH	262	-	1
2.	Co_3O_4-CeO_2	1M KOH	270	60	2
3.	CeO_2–CoO	1M KOH	296	76.78	3
4.	2 %Au/Ni_3N	0.1M KOH	280	52	4
5.	Ni_3N/NC	1M KOH	310	-	5
6.	Ni_3N@Ni-Ci NA/CC	1.0 M KHCO3	400	143	6
7.	Ptnanocluster@Ni_3N	1M KOH	285	57	7
8.	BGO/ Ni_3N	1M KOH	290	77.9	8
9.	Ni_3N/NiF	1M KOH	282	45	9
10.	Co-Ni_3N	1M KOH	270	94	10
11.	CeF_3-NiOOH	1M KOH	259	100	This work

Table S1. Table containing different catalysts for comparative study with CeF_3-NiOOH.

S3.2. ECSA normalized LSV curves of CeF_3-NiOOH, NiOOH and CeF_3:

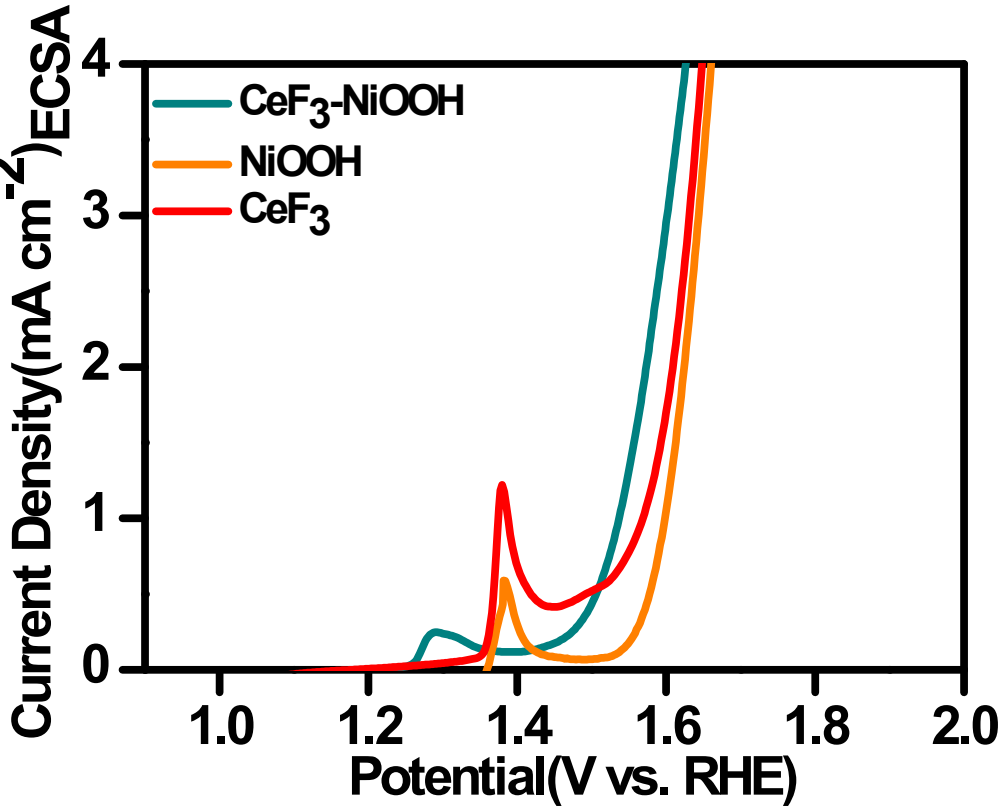

Figure S4. ECSA normalised OER activity of CeF_3-NiOOH, NiOOH and CeF_3

S3.3. Cyclic voltammetry curves of CeF_3-NiOOH, NiOOH and CeF_3 in non-faradic region:

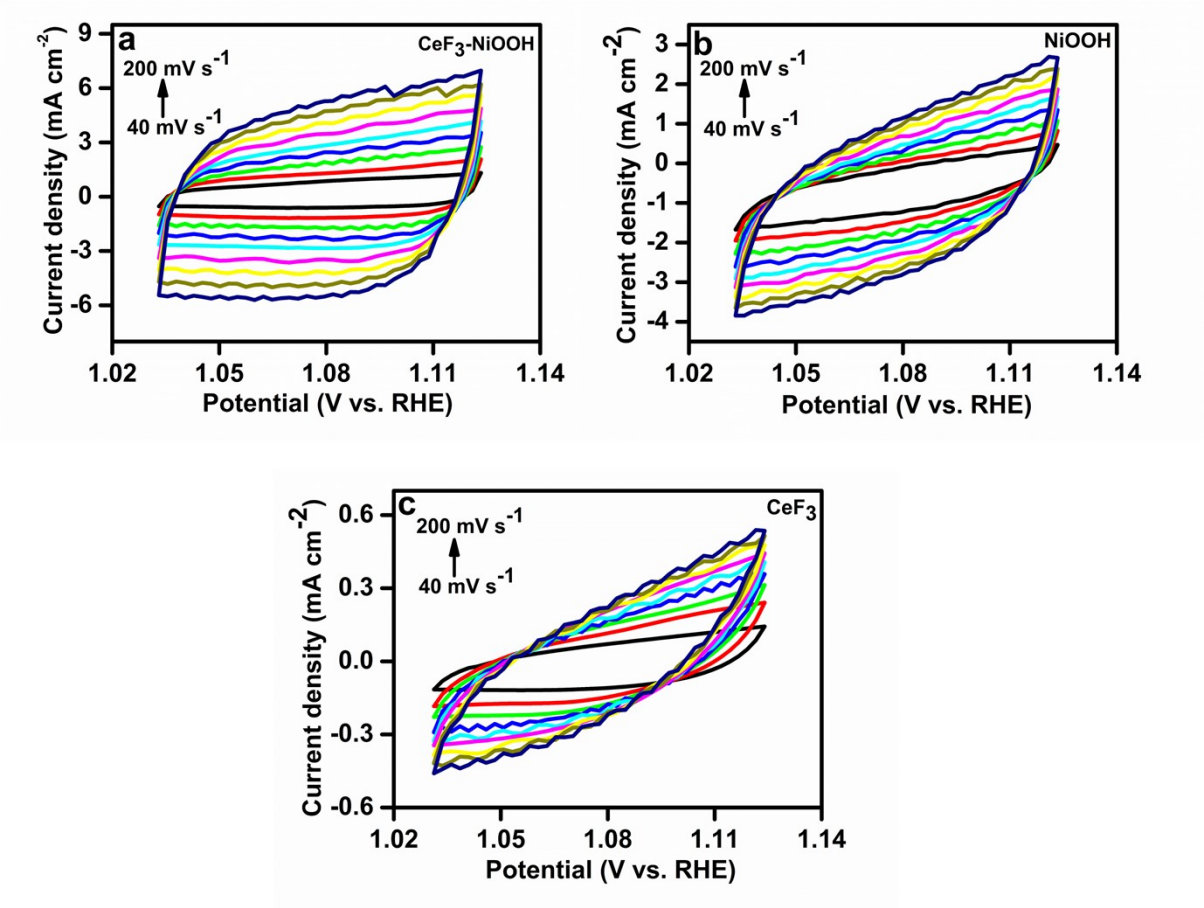

Figure S5. Cyclic voltammetry curves of CeF_3-NiOOH, NiOOH, and CeF_3 at different scan rates for the calculation of double-layer capacitance (C_{dl})

S3.4. After Stability data of CeF_3-NiOOH:

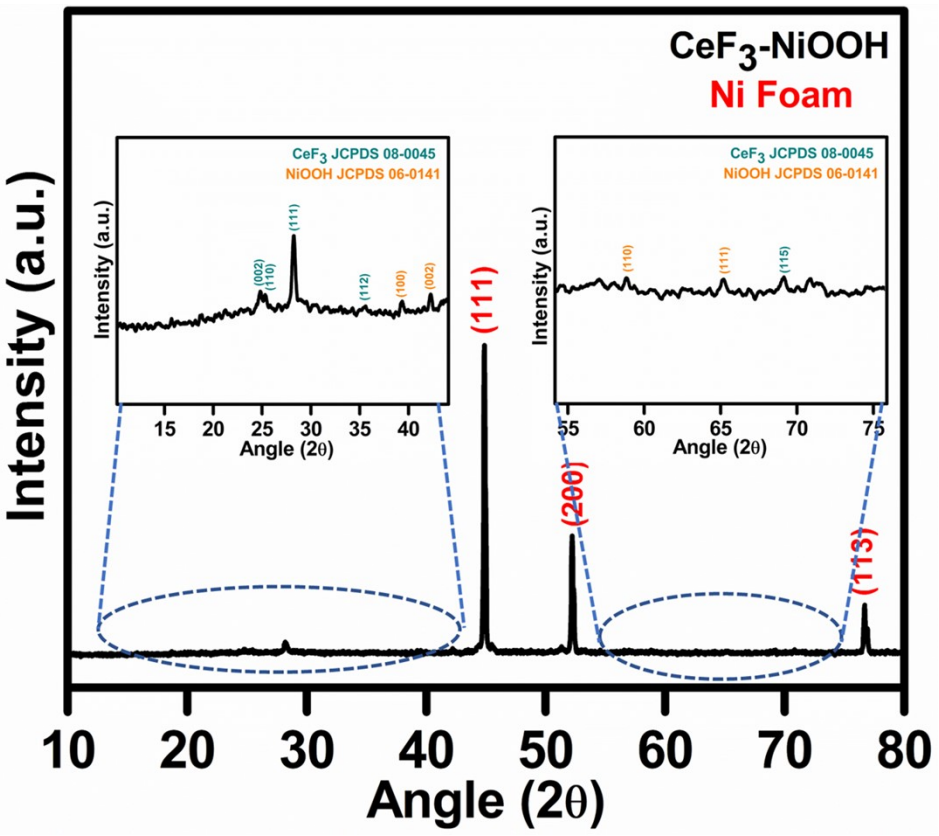

Figure S6. PXRD pattern of the CeF_3-NiOOH after stability

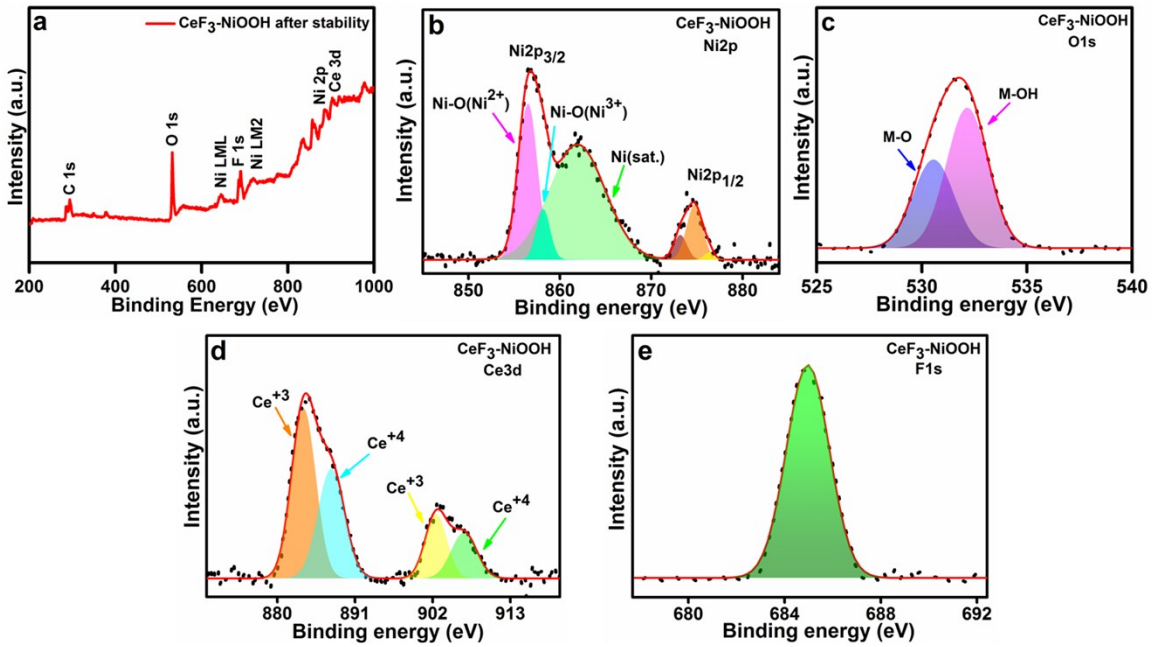

Figure S7. (a) XPS wide scan spectra of CeF_3-NiOOH after stability test, high resolution XPS spectra of (b) Ni2p (c) O1s (d) Ce3d and (e) F1s.

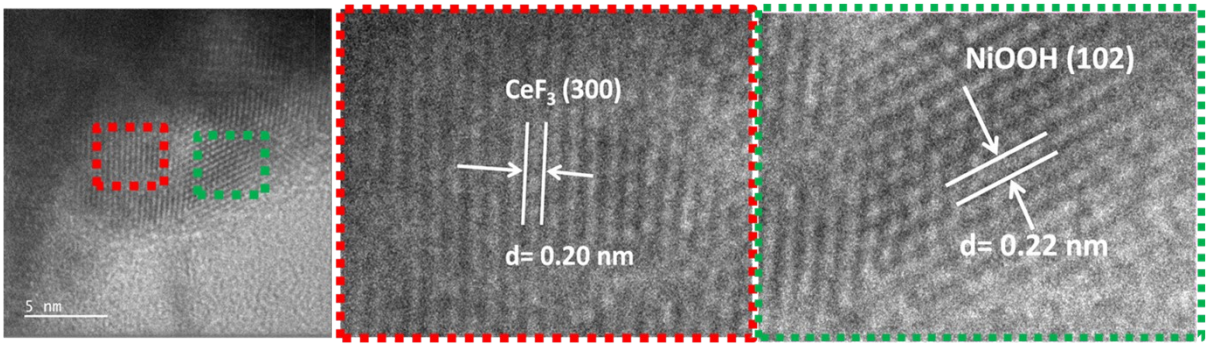

Figure S8. HRTEM images of CeF3-NiOOH after long term stability test

References: -

1. Kawashima, K., Márquez-Montes, R.A., Li, H., Shin, K., Cao, C.L., Vo, K.M., Son, Y.J., Wygant, B.R., Chunangad, A., Youn, D.H. and Henkelman, G., 2021. Electrochemical behavior of a Ni 3 N OER precatalyst in Fe-purified alkaline media: The impact of self-oxidation and Fe incorporation. *Materials Advances*, *2*(7), pp.2299-2309.
2. Liu, Y., Ma, C., Zhang, Q., Wang, W., Pan, P., Gu, L., Xu, D., Bao, J. and Dai, Z., 2019. 2D electron gas and oxygen vacancy induced high oxygen evolution performances for advanced Co3O4/CeO2 nanohybrids. *Advanced Materials*, *31*(21), p.1900062.
3. Li, W., Zhao, L., Wang, C., Lu, X. and Chen, W., 2021. Interface Engineering of Heterogeneous CeO2–CoO Nanofibers with Rich Oxygen Vacancies for Enhanced Electrocatalytic Oxygen Evolution Performance. *ACS Applied Materials & Interfaces*, *13*(39), pp.46998-47009.
4. Lv, M., Zhou, Y., Rasaki, S.A., Shen, H., Wang, C., Song, W., Thomas, T., Yang, M. and Wang, J., 2019. Gold Nanocluster-Decorated Nickel Nitride as Stable Electrocatalyst for Oxygen Evolution Reaction in Alkaline Media. *ChemElectroChem*, *6*(22), pp.5744-5749.
5. Chen, M., Qi, J., Guo, D., Lei, H., Zhang, W. and Cao, R., 2017. Facile synthesis of sponge-like Ni 3 N/NC for electrocatalytic water oxidation. *Chemical Communications*, *53*(69), pp.9566-9569.
6. Xie, F., Wu, H., Mou, J., Lin, D., Xu, C., Wu, C. and Sun, X., 2017. Ni3N@ Ni-Ci nanoarray as a highly active and durable non-noble-metal electrocatalyst for water oxidation at near-neutral pH. *Journal of Catalysis*, *356*, pp.165-172.
7. Pei, Y., Rezaei, B., Zhang, X., Li, Z., Shen, H., Yang, M. and Wang, J., 2020. Interface
8. catalysis by Pt nanocluster@ Ni 3 N for bifunctional hydrogen evolution and oxygen evolution. *Materials Chemistry Frontiers*, *4*(9), pp.2665-2672.
9. Li, B., Song, F., Qian, Y., Shaw, J. and Rao, Y., 2020. Boron-doped graphene oxide-supported nickel nitride nanoparticles for electrocatalytic oxygen evolution in alkaline electrolytes. *ACS Applied Nano Materials*, *3*(10), pp.9924-9930.
10. Tareen, A.K., Priyanga, G.S., Khan, K., Pervaiz, E., Thomas, T. and Yang, M., 2019. Nickel-based transition metal nitride electrocatalysts for the oxygen evolution reaction. *ChemSusChem*, *12*(17), pp.3941-3954.